

Expanded Gain-Switched Comb Source for 180 – 260 GHz Sub-THz Analog Radio-over-Fiber 6G Wireless System

Amol Delmade^{*1}, Cristian Vargas², Alison Kearney^{2,1}, Simon Nellen³, Robert B. Kohlhaas³, Martin Schell³, David Coffey², Frank Smyth² and Liam P. Barry¹

¹School of Electronic Engineering, Dublin City University, Dublin, Ireland, *amol.delmade2@gmail.com

²Pilot Photonics Ltd., Invent Center, Dublin City University, Dublin, Ireland

³Fraunhofer Institute for Telecommunications, Heinrich Hertz Institute (HHI), Berlin, Germany

Abstract: We demonstrate the successful generation and transmission of low-subcarrier spacing (up to 500 kHz) 6G compatible sub-THz OFDM signals in the 180 to 260 GHz frequency band using an expanded gain-switched laser comb source and waveguide-integrated photodiode antenna.

OCIS codes: (060.4510) Optical communications; (060.5625) Radio frequency photonics.

1. Introduction

Data transmission in the sub-THz (100-300 GHz) frequency bands will be an important aspect of the 6th generation (6G) wireless system to provide increased data rate to end users [1]. The combination of the optical heterodyne technique [2] and analog radio-over-fiber (ARoF) fronthaul link [3] can provide an efficient solution for the simultaneous generation and distribution of high-frequency sub-THz signals. In heterodyning, the beating of two optical carriers with a desired sub-THz carrier frequency difference is carried out on a high-speed photodetector. The ARoF fronthaul link distributes the data signal to the antenna sites by modulating it on optical carriers at an intermediate frequency (IF). The uncorrelated lasing frequency fluctuations and phase noise (PN) of free-running lasers limit their use in such optical heterodyne ARoF systems [4]— especially for the transmission of low subcarrier spacing (SC) orthogonal frequency division multiplexed (OFDM) signals synonymous with 5G. The use of frequency and phase-correlated carriers from an optical frequency comb (OFC) can lead to frequency-stable and low PN RF carrier generation [4] and the same is demonstrated here with an expanded gain-switched laser (GSL) comb.

The gain switching of a semiconductor laser provides a simple approach for the generation of OFCs with tunable free spectral range (FSR) and potential for photonic integration [4]-[6]. In the previous work in [6], we demonstrated a GSL OFC-based optical heterodyne ARoF link for the generation of millimeter wave signals up to 65 GHz frequency. However, the limited number of comb lines (typically 7-8 for >15 GHz FSR) hinder GSL OFC's use for the generation of high-frequency sub-THz signals. In this work, we demonstrate an expanded GSL OFC source with a 20 GHz FSR and ~280 GHz bandwidth (BW), stemming from 15 comb tones, without the need for an additional modulator. This source is used for sub-THz signal generation in the 180 - 260 GHz frequency range in combination with a waveguide integrated photodiode antenna (WIN-PD) from HHI [7] and WR4.3 waveguide-based sub-THz commercial receiver. In this work, we also analyze the PN of the generated sub-THz carriers and its effect on the performance of low SC spacing OFDM signals. In the previous sub-THz system demonstration based on GSL and phase modulator OFC [8], high baud rate single carrier data signal transmission was carried out for which the PN requirements are not that stringent. The PN of the heterodyne generated RF carriers typically increases with an increase in the spacing between the comb tones due to the nonlinear nature of the comb generation process. It is therefore important to analyze the PN for such high-frequency sub-THz carriers and its impact on the performance of the low SC spacing OFDM signals. Here, we varied the 200 MHz bandwidth OFDM signals SC spacing from 4 MHz to 250 kHz and analyzed its performance at 200 and 240 GHz frequencies generated over a 10 km optical heterodyne ARoF link. To the best of our knowledge, this is the first low SC spacing 6G compatible OFDM data signal generation and distribution demonstration at high-frequency sub-THz frequencies with an OFC source.

2. Experimental Setup and Details

The schematic of the optical heterodyne ARoF system based on expanded GSL OFC is shown in Fig. 1 along with figurative spectra. Two DFB lasers (>18 GHz BW) with slightly different lasing frequencies were gain-switched using a 20 GHz RF sinusoidal signal such that a few tones from the individual generated combs overlap in frequency [9]. A ~50 kHz low linewidth external cavity master laser, with the lasing frequency close to the overlapping tones of two GSL OFCs, was injected into these lasers, as shown in inset (i) in Fig. 1, to correlate the phase and frequency of these combs with each other [9]. The optical spectrum of the expanded comb is shown in inset (ii) of Fig. 1 with 15 lines within 10 dB flatness. A programmable wavelength selective switch (WSS) was used to filter out two OFC tones

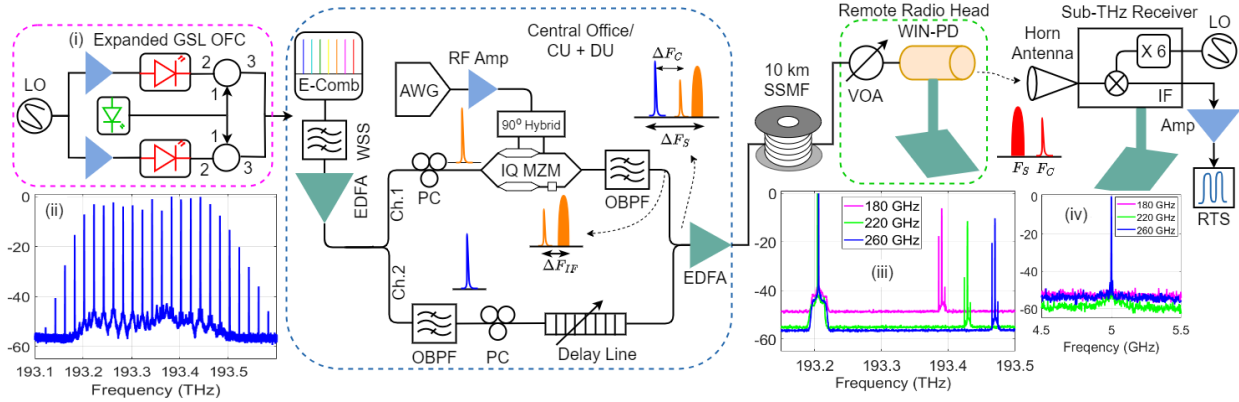


Fig. 1 Optical heterodyne ARoF Sub-THz wireless system using an expanded GSL OFC and WIN-PD. The insets (i) and (ii) show the architecture and optical spectra of the expanded GSL-OFc; (iii) shows the optical spectrum at the input of SSMF and (iv) shows IF spectrum of the frequency down-converted sub-THz signals, respectively, for 180, 220 and 240 GHz cases.

separated by 180 to 260 GHz frequencies (ΔF_c) for use in heterodyning for sub-THz signal generation. An Erbium-doped fiber amplifier (EDFA) was used to boost the power of these tones before splitting them into two paths.

200 MHz BW OFDM data signal at an IF of 4.5 GHz (F_{IF}) was initially single sideband modulated on one of these optical carriers in channel 1 using a 90° hybrid and IQ Mach-Zehnder Modulator (IQ-MZM) as shown in Fig. 1. The OFDM signals with variable SC spacing were generated and frequency converted to the IF in Matlab and the samples were loaded into an arbitrary waveform generator (AWG) to convert it into an electrical signal. In order to keep the OFDM signal BW constant for different SC spacing, the IFFT size and number of data subcarriers were changed by a factor of two with respect to the previous SC spacing signal. The bias of IQ-MZM was adjusted to minimize the power in the carrier. Optical bandpass filters were used in both channel paths to remove the unwanted frequency components before combining the signals. The spectrum of the combined signal consisting of an unmodulated carrier, remaining modulated carrier and a modulated data signal, 4.5 GHz away, is shown in Fig. 1(iii) for the cases of 180, 220 and 260 GHz sub-THz signal generation. The frequency of the unmodulated carrier was kept the same and different OFC tones were selected for data modulation and subsequent sub-THz signal generation. The combined signal was transmitted through a 10 km standard single-mode fiber (SSMF) after amplification by EDFA.

At the remote unit antenna site, a variable optical attenuator (VOA) was used to control the power incident on the WIN-PD THz transmitter consisting of an InP-based photodiode with integrated bowtie THz antenna [7]. The WIN-PD transmitter is designed for broadband CW radiation generation up to 4.5 THz and has a silicon lens for radiating into free space. The emitted THz power reaches a peak value of $340 \mu\text{W}$ at 115 GHz and falls off to $\sim 1 \mu\text{W}$ at 1 THz [7]. The photo-mixing of the three optical components from the combined signal on the WIN-PD results in the generation of a sub-THz data signal between 180 to $260 + 4.5$ GHz (F_c) and sub-THz carrier between 180 to 260 GHz (F_c). The emitted signal was captured by the horn antenna of the sub-THz receiver consisting of a WR 4.3 waveguide-based mixer which down-converted the sub-THz signal to the IF. The LO carrier for the mixer was generated using a 6-time frequency multiplier inside the Virginia Diode receiver box as shown in Fig. 1. The frequency of the LO feed to the multiplier was changed accordingly to down-convert the captured sub-THz signals to 4.5 GHz IF. The spectrum of frequency down-converted IF carriers is shown in Fig. 1(iv). The use of WR 4.3 waveguide limited the frequency of operation in the 170 – 260 GHz band, while the absence of collimating lenses and amplifiers at such a high-frequency range limited the wireless transmission distance to 0.5 m. The IF signal was captured using a real-time scope (RTS) and offline processing was done using Matlab to demodulate the signal and analyze its error vector magnitude (EVM) performance.

3. Results and Discussion

Initially, we filtered different sets of OFC tones from an expanded GSL and analyzed the system performance at different sub-THz frequencies from 180 to 260 GHz for the transmission of 200 MHz BW OFDM signal with SC spacing of 4 MHz and a raw data rate of 1.2 Gb/s. The results for back-to-back (B2B) and 10 km transmission (at two different received optical powers) are shown in Fig. 2(i) along with a few constellation diagrams. The launch power into the fiber was kept constant at 11 dBm and VOA was used to change the power falling on WIN-PD. The frequency range limitation stems from the use of a WR 4.3 waveguide in the sub-THz receiver. The results for B2B transmission at 8 dBm received optical power on WIN-PD show less than 1.25 % EVM variation as the sub-THz signal's frequency is tuned over the 80 GHz range. This variation stems from the non-ideal frequency response of the various components used in the system and the variation in the carrier-to-noise ratio for different comb tones used for sub-THz signals

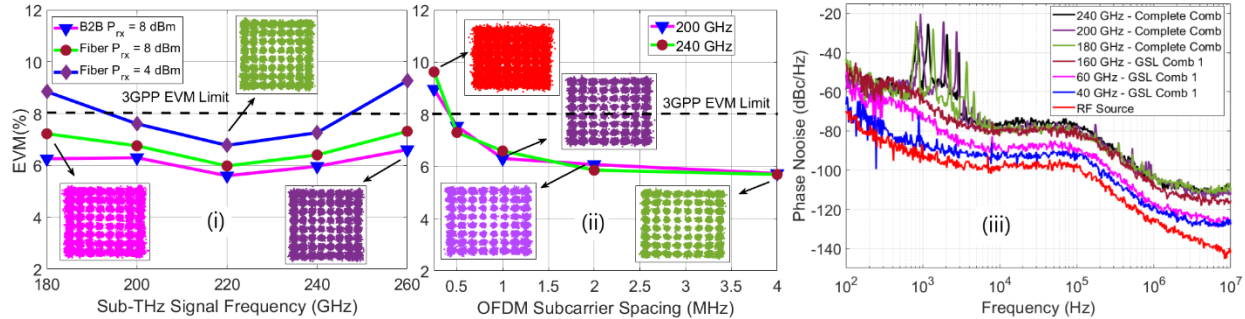


Fig. 2 (i) EVM vs sub-THz frequency and (ii) EVM vs SC spacing performance for OFDM signals and (iii) Phase noise of generated sub-THz carriers over an optical heterodyne analog RoF system employing an expanded GSL OFC and WIN-PD.

generation. Approximately 1% EVM penalty is observed upon 10 km fiber transmission due to nonlinear effects in fiber with higher launch power. Nevertheless, the performance of 64-QAM data-modulated OFDM signals was below the 3GPP EVM limit of 8% for all the frequencies at 8 dBm received power - showing the flexibility and robustness of the system to generate variable frequency sub-THz signals. As the optical power on WIN-PD is reduced to 4 dBm, the performance of 180 and 260 GHz signals went above the 3GPP limit due to the reduction in signal-to-noise ratio. The inset constellation diagrams in Fig. 2(i), with less than 8% EVM indicate the successful sub-THz signal generation and transmission over a 10 km optical heterodyne ARoF link resulting in OFDM data transmission rate of 1.2 Gb/s.

In the second part, the outlined sub-THz system performance is analyzed for variable SC spacing OFDM signal transmission at 200 and 240 GHz frequencies for the B2B transmission. The results, shown in Fig. 2(ii), indicate performance degradation as the SC spacing is reduced from 4 MHz to 250 kHz, however the 500 kHz SC spacing is still below the 3GPP limit. This degradation stems from the higher PN of the generated sub-THz carriers than that required for error-free transmission of low SC spacing multicarrier signals. We also measured the PN of sub-THz carriers after frequency down-conversion to IF and the results are shown in Fig. 2(iii). As the spacing between the comb tones increases the PN of the generated carriers increases as seen from the plots for 40, 60 and 160 GHz carriers (from a single gain-switched laser). However, in the case of 180, 200 and 240 GHz sub-THz carriers the PN is observed to be almost the same as the optical carriers for heterodyning were obtained from the expanded comb consisting of two gain-switched lasers both locked with a single master laser. The 200 and 240 GHz generated carriers have a PN below -75 dBc/Hz and -100 dBc/Hz at 10 kHz and 10 MHz offset from the carrier, respectively. The spurious peaks in the PN around 1 kHz offset emanate from the imperfect isolation and crosstalk between the gain-switched lasers. These PN values are still sufficiently low to successfully demodulate 500 kHz and higher SC spacing OFDM signals as seen by the below 3GPP limit EVM performance in Fig. 2(ii). These results show that the expanded GSL OFC-based optical heterodyne ARoF system is capable to successfully generate and transmit the 6G compatible (480 kHz and higher) SC spacing OFDM signals in the sub-THz band. The ability to develop a photonic integrated circuit of the entire transmitter can lead to wide deployment of such links for the 6G systems operating in the sub-THz band. The potential of further expanding the comb with an additional phase modulator or dual drive MZM stage can lead to the expanded GSL OFCs use in THz carrier generation with more than 300 GHz frequency.

4. Conclusion

Frequency-stable and low-phase noise sub-THz carrier generation is paramount for a simple and cost-efficient 6G wireless system implementation capable of transmitting low subcarrier spacing multicarrier signals. The system presented here based on the expanded gain-switched laser OFC and waveguide integrated photodiode antenna successfully demonstrates the generation and transmission of sub-THz OFDM signals in the 180 - 260 GHz frequency band. The low PN of the generated carriers from the heterodyne system supports the transmission of 6G compatible OFDM signals with SC spacing well down to 500 kHz – showing its potential for field deployment. The possibility of photonic integration of most of the components and increasing the comb bandwidth can further reduce the complexity and cost of such a system and increase its use cases.

Acknowledgment

This work has emanated from research grants from Science Foundation Ireland (SFI), co-funded under the European Regional Development Fund grants 13/RC/2077, 12/RC/2276_P2 and European Space Agency grants 4000138240/22/NL/GLC/my, 4000139033/22/NL/IB/gg.

References

- [1] T. S. Rappaport *et al.*, *IEEE Access*, vol. 7 (3), pp. 78729-78757, 2019.
- [2] X. Pang *et al.*, *JLT*, vol. 40(10), pp. 3149-3162, 2022.
- [3] C. Lim *et al.*, *JLT*, vol. 39(4), pp. 881-888, 2021.
- [4] C. Browning *et al.*, *JLT*, vol. 36(19), pp. 4602-4610, 2018.
- [5] M. D. G. Pascual *et al.*, *IEEE PJ*, vol. 9(3), pp. 1-8, 2017.
- [6] A. Delmède *et al.*, *Elsevier JOC*, vol. 545, 129681, 2023.
- [7] S. Nellen *et al.*, *JIMTW*, vol. 41, pp. 343-354, 2020.
- [8] H. Shams *et al.*, *IEEE PJ*, vol. 7(3), pp. 1-11, 2015.
- [9] Prajwal D. L. *et al.*, *MDPI Applied Sciences*, vol. 11(15), 2021.